Title:	The Effects of High-Altitude Nuclear Explosions on Transmission Grids
Author(s):	Barnes, Arthur K.
Intended for:	Report
Issued:	2019-03-07

The Effects of High-Altitude Nuclear Explosions on Transmission Grids

Barnes, Arthur K | Los Alamos National Laboratory | March 1, 2019

I. Introduction

Assessing impact of high-altitude electromagnetic pulses (HEMP) resulting from the effects of nuclear weapons is a problem of great concern. Some previous studies have estimated the extent and duration of an outage to be severe. In this report, we quantify the extent and duration of an outage resulting from HEMP E1 to the best of our ability given existing knowledge and tools. Our analysis focuses on the impact to civilian consumer of electricity as opposed to the impact on military responsiveness.

A. E1 COUPLING DAMAGE

The mechanism by which HEMP E1 causes damage to the electric transmission network is by coupling into the voltage transformer measurement lines of protective relays. This results in a high voltage pulse appearing on the relay voltage transformer input terminals, which can cause the relay to enter an inoperable state or be permanently damaged. It is possible for this pulse to cause a relay misoperation, though this is unlikely. The details of this process are described in [1]. The likelihood for damage depends on the measurement line and cable type. For this study, we assume that the distribution of measurement line orientations is uniform. This leads to a bus outage probability of roughly 50%.

B. POWER SYSTEM DAMAGE RESPONSE

A qualitative illustration of the response of an electric power system to a disaster event such as a hurricane, earthquake or HEMP is presented in Figure 1. In the pre-contingency stage, the system is subjected to stress such as the loss of lines as transmission towers are toppled by a hurricane or substation buses are disabled from EMP damaging protective and control equipment in substation control houses. This stage may lead to a cascading failure in which generation capability is rapidly lost as protective devices activate. A number of different interactions between diverse power systems components cause positive feedback in the system until a total blackout results, or operable portions of the system are left islanded. In the recovery period, the system or inoperable portions of the system are black-started and generators are re-dispatched so that a portion of load can be served. Finally, line crews sent to the affected area are able to repair or replace components so that over time all or almost all load power is restored.

Modeling the cascading portion of the damage response is a challenging problem on account of both the computational complexity and data requirements [2], [3]. In the case of a deliberate attack it may be necessary to predict the peak load lost in order to evaluate the ability of the military to respond to the threat. For this report, we focus on the impact to civilian electricity customers. Widespread outages on the order of a day are not especially harmful to civilian customers, as most municipalities anticipate shutting down every few years in the case of severe snowstorms. In this report, we focus on analyzing the ability of the electric power system to provide power during the restoration period, as this will dominate the economic impact [4].

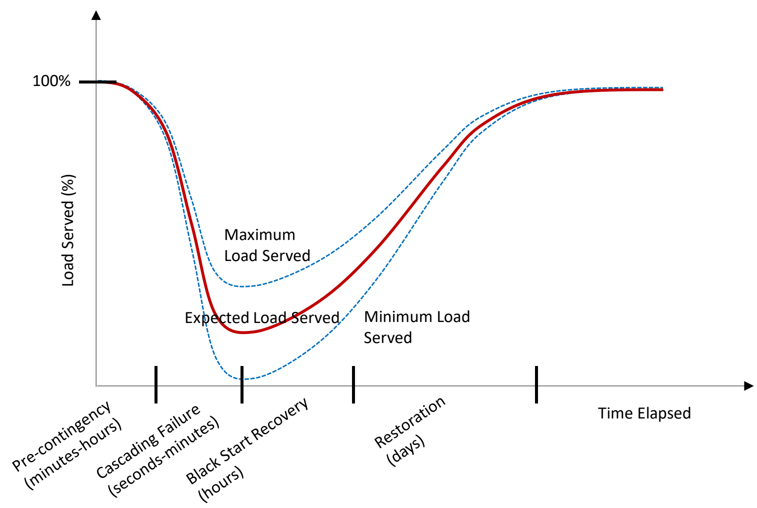

Figure 1. Response over time of an electric power system to a disaster event.

C. MITIGATION AND RESTORATION

Los Alamos National Laboratory has not been contracted at this point to perform analysis of transmission system restoration for HEMP events. Therefore, this report will focus on subject matter expertise to estimate the restoration timeline as opposed to quantitative analysis such as described in academic literature [5].

For mitigating the impact of HEMP on protective relays, it is necessary to disconnect them from voltage transformer lines. However, it is current practice that such lines are connected to the back of the relay enclosure via screw terminals and there are no disconnect switches or quick releases for the protective relays. Furthermore, given the spatial dispersal of substations, it is unlikely that such mitigation is feasible to perform given the amount of advance warning anticipated.

For restoration, it is fortunate that not all inoperable relays need to be replaced in order to supply power. It is current practice to operate protective relays with several zones of protection so that a transmission line can be protected from faults by relays and breakers at substations on adjacent transmission lines [6]. Operating the system in such a manner will result in a loss of selectivity of protection as a fault will result in several transmission lines being disconnected.

Replacement of damaged relays is complicated by the fact that relays can come in horizontal or vertical form factors. For a line relay, configuration options can include the current transformer rated current, supply voltage and single-phase or three-phase tripping.

Based on these observations and the ability of unaffected utilities to provide aid in the form of spare equipment and line crews, we estimate that the majority of load lost should be recovered within weeks, but a more detailed estimate of the timeline is not possible.

II. Problem Formulation

To assess the impact of E1 EMP on an electric transmission system the SCS is employed [7]. A random subset of buses is disabled to generate a contingency following the approach described in [8], but with bus outages instead of branch outages. Additionally, while [8] aims to capture the relationship between variation in load shed and network properties, this study estimates the relationship between amount of load shed and fraction of buses disabled on representative portions of the continental USA electric transmission system. SCS is run on both the unmodified system and on the contingency system using the second-order-cone relaxation [9]–[12], which provides an upper bound in terms of load served. The load shed is measured as the ratio of load served in the damaged system over the load served in the unmodified system. This is described in Model 3 of [12], which is summarized in eqs. (1)−(10).

$$max. \sum_{i \in N} z_i^v, \sum_{i \in N} z_i^g, \sum_{i \in N} z_i^s, \sum_{i \in N} \left|\mathcal{R}e\left(S_i^d\right)\right| z_i^d \tag{1}$$

s.t.

$$\left|S_{ij}\right| \leq S_{ij}^u \forall (i,j) \in E \cup E^R \tag{2}$$

$$z_i^g S_i^{gl} \leq S_i^g \leq z_i^g S_i^{gu} \forall i \in N \tag{3}$$

$$z_i^v \left(V_i^l\right)^2 \leq W_{ii} \leq z_i^v (V_i^u)^2 \quad \forall i \in N \tag{4}$$

$$W_{ii}^s = \langle z_i^s W_{ii} \rangle^M \quad \forall i \in N \tag{5}$$

$$S_i^g - z_i^d S_i^d - Y_i^s W_{ii}^s = \sum_{(i,j) \in E \cup E^R} S_{ij} \quad \forall i \in N \tag{6}$$

$$S_{ij} = \left(Y_{ij}^* - \boldsymbol{i} \frac{b_{ij}^c}{2}\right) \frac{W_{ii}}{\left|T_{ij}\right|^2} - Y_{ij}^* \frac{W_{ii}}{T_{ij}} \; (i,j) \in E \tag{7}$$

$$S_{ji} = \left(Y_{ij}^* - \boldsymbol{i} \frac{b_{ij}^c}{2}\right) \frac{W_{jj}}{\left|T_{ij}\right|^2} - Y_{ij}^* \frac{W_{ii}}{T_{ij}} \; (i,j) \in E \tag{8}$$

$$tan\left(-\theta_{ij}^{\Delta}\right) \mathcal{R}e\left(W_{ij}\right) \leq \mathcal{I}m\left(W_{ij}\right) \leq tan\left(\theta_{ij}^{\Delta}\right) \mathcal{R}e\left(W_{ij}\right) \tag{9}$$

$$\left|W_{ij}\right|^{\Delta} \leq W_{ii} W_{jj} \forall (i,j) \in E \tag{10}$$

Equation (1) describes a multi-objective where z_i^g and z_i^v are on-off variables for generator and bus statuses, while z_i^d and z_i^s are continuous variables over [0,1] that model load shedding. The complex variables S_{ij}, S_i^g and S_i^d are the branch power flows, generator power and load power demands respectively at bus i, where N is the set of buses in the network. In (2) S_{ij}^u is the thermal limit of branch (i,j) while E and E^R are the sets of "from" and "to" edges in the network. In (3) S_i^{gl} and S_i^{gu} are the lower and upper bounds of the generator at bus i. In (4) V_i^l and V_i^u are the lower and upper voltage limits at bus i, where $W_{ij} = V_i V_j^*$. For the special case $i = j$, $W_{ii} = |V_i|^2$. In (5) $\langle x, y \rangle^M$ represents the McCormick envelope of x and y. Equation (6) represents power balance at each node. Equations (7) and (8) represent power flow into the sending and receiving end of each branch, where T_{ij} is a complex variable representing the change in voltage magnitude and phase across any transformer branches, and b_{ij}^c represents the charging capacitance of line branches. Equation (9) limits the change in voltage phase angle across any branch to be between $-\theta_{ij}^{\Delta}$ and $+\theta_{ij}^{\Delta}$. Last, (10) is a convex rotated second-order-cone constraint.

III. Case Studies

The impact of HEMP is investigated with two case studies: an ERCOT model and an equivalenced model of the Eastern Interconnect (EI) centered around Tennessee. SCS limits the case study systems to less than approximately 10^4 buses, preventing the use of the entire EI. For both systems SCS is run while sweeping the fraction of disabled buses from 6.25% to 50%. In both sweeps two scenarios are considered: first, disabling buses throughout the entire modeled system, and second, disabling buses only in a specific geographic region. The second scenario captures the reduction in load lost resulting from the spared portion of the network helping to supply load. For both scenarios, 1,000 different damage instances are generated and SCS is run on them.

The ERCOT model is based on a 2015 FERC filing, and includes 6,648 buses. It is illustrated in Figure 2. For the mixed damaged/spared scenario only the northern 3,362 buses of the system north of 31.5° N latitude (illustrated in red) are damaged. The resulting load shed for both scenarios is illustrated in Figure 3. Surprisingly, the percentage of load shed within the damaged region is very similar for both scenarios across all damage percentages. This indicates that the spared region is unable to provide power to a significant number of loads within the damaged region. In both scenarios the percentage of load shed grows approximately linearly at twice the rate of the percentage of buses disabled, so for a 50% damage scenario the network is mostly inoperable.

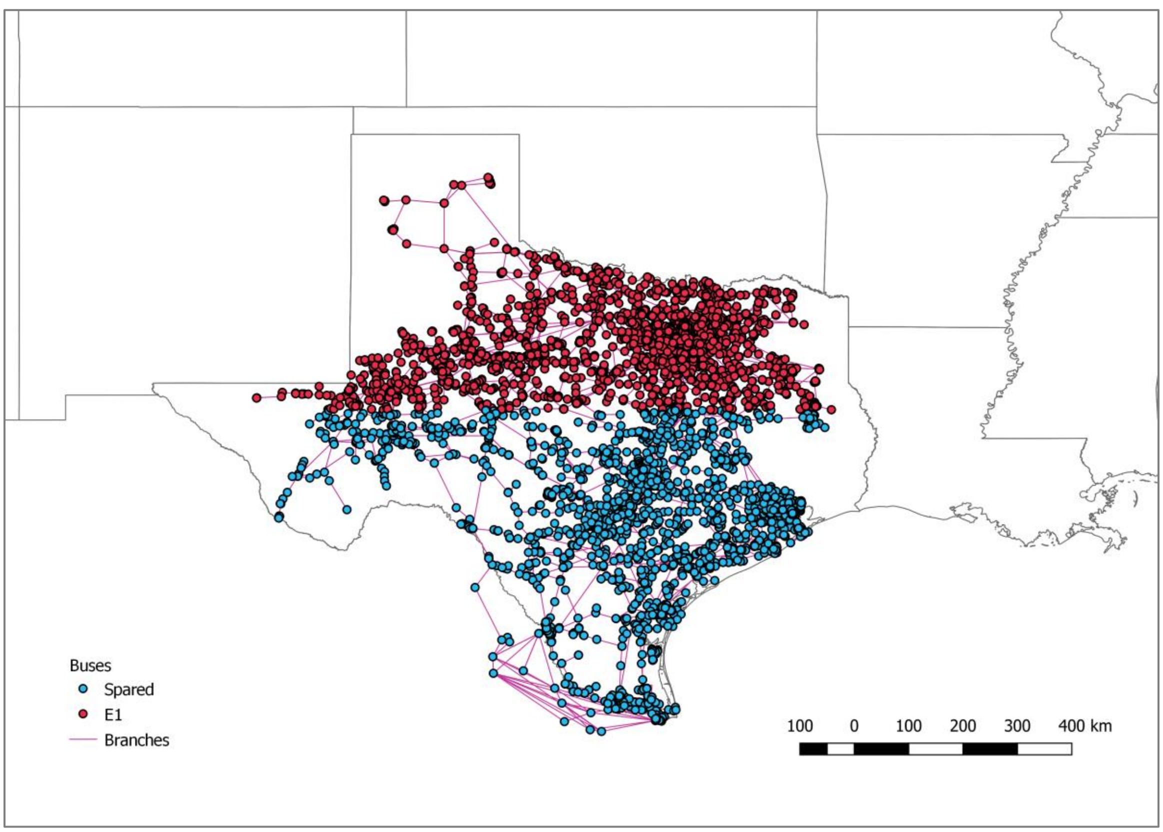

Figure 2. ERCOT system showing disabled (north) and spared (south) portions.

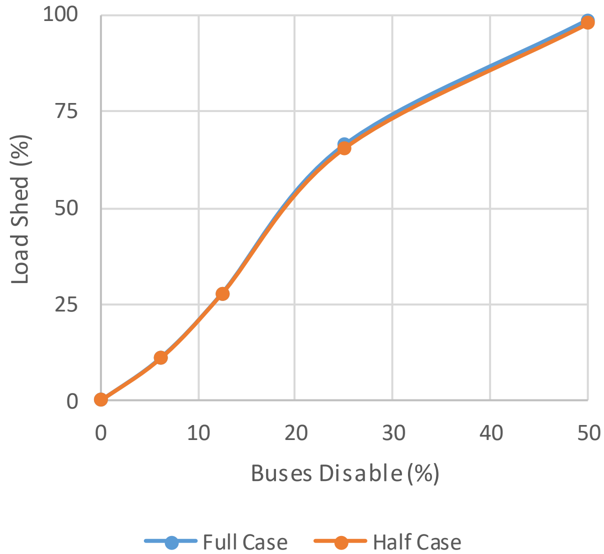

Figure 3. Load shed vs. percentage of buses disabled for the ERCOT case.

The EI model is based on a 2009 FERC filing that includes 54,634 buses. The Ward equivalencing method from PowerWorld [13] is employed to reduce this down to a disk 3.5° in diameter centered around a point (−83.85, 34.9) in Tennessee with 5,720 buses. Within this equivalenced region, an interior region of 2° in diameter with 1,306 buses is damaged. The two concentric regions are illustrated in Figure 4, while the percentage load shed vs. percentage of buses is illustrated in Figure 5. In this case, the partially damaged scenario shows a noticeable but small reduction in load shed.

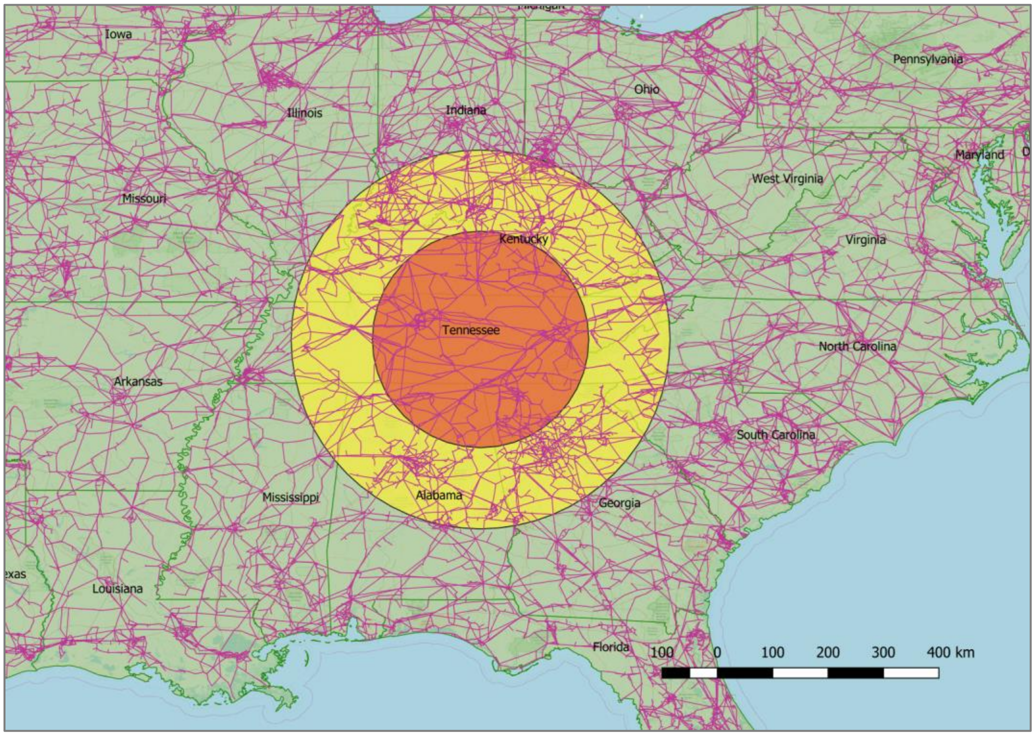

Figure 4. Eastern Interconnect (EI) system showing equivalence region (yellow) with disabled region (orange).

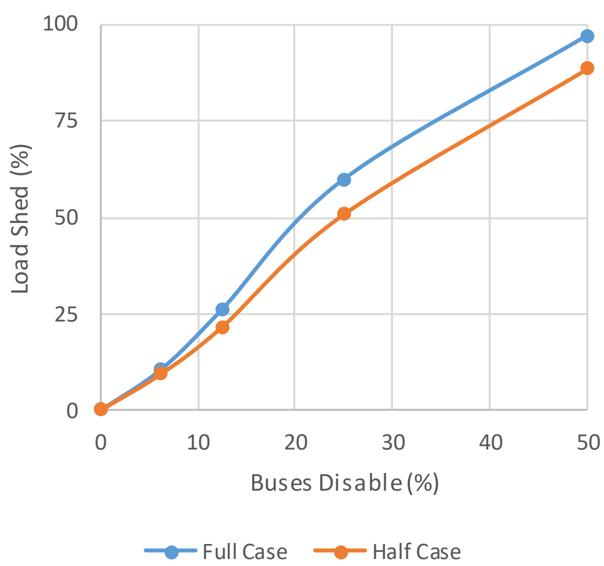

Figure 5. Measured load shed for the EI subset.

IV. Conclusions

In the event of relay damage caused by HEMP E1 resulting in buses being removed from service, there is a roughly linear relationship between the percentage of disabled buses and load loss, with 50% of buses disabled resulting in a majority of load lost within the network. Although investigating methods to improve the resilience of relaying to E1 damage is recommended, we do not have specific recommendations for best practices. Without hardening substation equipment, it is unlikely that there are practical short-term procedures to reduce the likelihood of damage. Although we are currently unable to model the progression of cascading events, for evaluating the impact to civilian consumers it is only necessary to model the load lost in the restoration period which can last over a week, as opposed to the peak load shed, which in anticipated to last only for hours to a day, after which time utilities are able to black-start the undamaged portions of their systems. Replacing relays can be involved as on account of the large number of damaged relays it will likely not be possible to replace all of them with exact matches. This will create some difficulty in terms ensuring that the protection settings are not changed, in addition to the possible need to modify the substation panel to accommodate a relay with a different form factor. However, this is mitigated by the fact that utilities will not need to replace all damaged relays. Instead, a fraction can be replaced at a loss of protection selectivity.

V. References

[1] R. Horton, "Coupling of early-time high-altitude electromagnetic pulse (E1) into technological infrastructure," Electric Power Research Institute (EPRI), 2018.

[2] M. Vaiman *et al.*, "Risk assessment of cascading outages: Part I — Overview of methodologies," in *2011 IEEE Power and Energy Society General Meeting*, 2011, pp. 1–10.

[3] P. D. H. Hines, I. Dobson, E. Cotilla-Sanchez, and M. Eppstein, "'Dual Graph' and 'Random Chemistry' Methods for Cascading Failure Analysis," in *2013 46th Hawaii International Conference on System Sciences*, 2013, pp. 2141–2150.

[4] A. K. Barnes, B. K. Edwards, M. Ewers, A. W. McCown, and S. Backhaus, "Western CONUS Power Outage: Electric Power, Infrastructure, and Economic Analysis," Los Alamos National Laboratory, LA-CP-18-20280, May 2018.

[5] C. Coffrin and P. V. Hentenryck, "Transmission System Restoration: Co-optimization of repairs, load pickups, and generation dispatch," in *2014 Power Systems Computation Conference*, 2014, pp. 1–8.

[6] J. Lewis. Blackburn, *Protective Relaying Principles and Applications, Third Edition.*, 3rd ed. Hoboken: Taylor & Francis, 2007.

[7] C. Coffrin, R. Bent, B. Tasseff, K. Sundar, and S. Backhaus, "Relaxations of AC Minimal Load-Shedding for Severe Contingency Analysis," *ArXiv171007861 Math*, Oct. 2017.

[8] M. R. Kelly-Gorham, C. Coffrin, A. Barnes, and P. D. H. Hines, "Identifying Transmission Network Properties That Impact System Vulnerability," presented at the Power and Energy Society General Meeting, In Review, Atlanta, 2019.

[9] C. Coffrin, H. L. Hijazi, and P. Van Hentenryck, "The QC Relaxation: Theoretical and Computational Results on Optimal Power Flow," *ArXiv150207847 Cs Math*, Feb. 2015.

[10] C. Coffrin, H. L. Hijazi, and P. Van Hentenryck, "Network Flow and Copper Plate Relaxations for AC Transmission Systems," *ArXiv150605202 Cs Math*, Jun. 2015.

[11] R. A. Jabr, "Radial distribution load flow using conic programming," *IEEE Trans. Power Syst.*, vol. 21, no. 3, pp. 1458–1459, Aug. 2006.

[12] B. Subhonmesh, S. H. Low, and K. M. Chandy, “Equivalence of branch flow and bus injection models,” in *2012 50th Annual Allerton Conference on Communication, Control, and Computing (Allerton)*, 2012, pp. 1893–1899.

[13] J. B. Ward, “Equivalent Circuits for Power-Flow Studies,” *Trans. Am. Inst. Electr. Eng.*, vol. 68, no. 1, pp. 373–382, Jul. 1949.